SDSS'Rio 2010 STABILITY AND DUCTILITY OF STEEL STRUCTURES
E. Batista, P. Vellasco, L. de Lima (Eds.)
Rio de Janeiro, Brazil, September 8 - 10, 2010

EXPERIMENTAL ANALYSIS OF COMPOSITE CONNECTIONS USING SLAB MADE BY PRECAST JOIST WITH LATTICE AND BRICKS

William Bessa*, Roberto M. Gonçalves*, Carlo A. Castiglioni and Luis Calado*****

* Escola de Engenharia de São Carlos, EESC – USP, São Carlos, Brazile-mails: willbessa@gmail.com, goncalve@sc.usp.br
** Politecnico di Milano, Milan, Italy
e-mail: castigli@stru.polimi.it

*** Instituto Superior Tecnico, Lisbon, Portugal
e-mail: calado@civil.ist.utl.pt

Keywords: Composite Connections, Precast Joist, FEM Modeling, Slab Cracking.

Abstract. *This research presents an experimental study of steel concrete composite connections with bottom and web angle. It was tested 4 full-scale specimens (2 single-sided and 2 double-sided composite connections), with 0,2% and 1% for the secondary steel ratio. The specimens were fabricated with precast concrete slabs with steel joist (predalles) and bricks infill, a constructive technique widely used in Brazil. The experimental studies of isolated specimens were a previous step for the typical floor composite connections analysis. The main objectives were to evaluate the concrete slab cracking on the behavior of composite connections (initial stiffness and resistant moment) and the secondary steel ratio increase. The experimental results were compared with numerical models, using FEM, with the goal of including the longitudinal and transversal steel bars, concrete slab, geometrical and material non linearity. Comparisons between numerical and experimental results showed satisfactory agreement and indicated the connection failure mode for the ultimate limit states.*

1 INTRODUCTION

The steel-concrete composite construction has increased in engineering practice, especially in composite frames for buildings that consist of steel concrete composite beams and steel columns. This type of composite frame has several structural and constructional advantages, such as good fire resistance and high strength, large stiffness and ductility, local and global buckling restraints on steel beams provided by concrete slabs, and reduced construction costs.

The stiffness and strength of steel frames can be significantly increased by a composite concrete slab in beams. This can be achieved by providing a few continuous reinforcing steel bars across the column lines and ensuring full or partial composite action through the use of shear connectors - Li et al. (1996) [1].

Design procedures for steel and composite connections have been modified during the last three decades in order to incorporate the semi-rigid connection behavior into the frame design process. The 3D numerical modeling of the real connections behavior leads to more reliable designs and economy in civil construction.

This paper presents an experimental study of steel concrete composite connections with bottom and web angle. It was tested 4 full-scale specimens (2 single-sided and 2 double-sided composite connections) with precast concrete slabs with steel joist (predalles) and bricks infill. The experimental results were compared with numerical models, using FEM, with the goal of including the concrete slab, shear connectors, longitudinal and transversal steel bars, material nonlinearities, geometrical discontinuities and large displacements.

2 EXPERIMENTAL PROGRAM

The experimental program was carried out by Bessa (2009) [2], at the São Carlos Engineering School of University of São Paulo (EESC-USP), for beam-to-column composite connections with bottom and web angle. It was tested 4 specimens (2 single-sided and 2 double-sided composite connections) with monotonic loading. It was considered specimens with 0,2% and 1% for the secondary steel ratio, and 1% for the longitudinal steel bars ratio.

The Table 1 shows the specimens tested with their respective main definitions: ***RSS = 1%*** and ***NRSS = 0,2%*** for the transversal steel bars ratio.

Table 1: Specimens tested.

Prototype	Connection	Longitudinal steel bars ratio	Transversal steel bars ratio
TNRSS	Simple sided	1%	0.2%
TRSS	Simple sided	1%	1%
CNRSS	Double sided	1%	0.2%
CRSS	Double sided	1%	1%

The Figure 1 illustrates the geometrical characteristics for the single sided and double sided specimens. The Table 2 indicates the connection components characteristics, with standard rolled steel beams and column, bolts with 19mm and 16mm (for column major and minor axis connections, respectively), angles (bottom and web) and shear connectors characteristics.

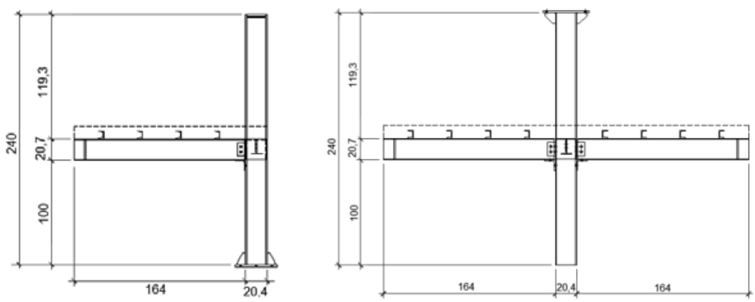

Single sided specimens (cm). Double sided specimens (cm).

Figure 1: Specimens geometrical characteristics.

Table 1: Specimens tested.

Element	Characteristics
Composite beam	W 350 x 13 kgf/m
Column	HP 200 x 53 kgf/m
Shear Connectors	U 75x50x7,5mm
Bolts – column major axis	ASTM A324 – ϕ19mm
Bolts - column minor axis	ASTM A324 – ϕ16mm
Bottom angle	L 4“ x 4“ x 5/16“
Web angle	L 3“ x 3“ x 1/2“
Steel longitudinal bars	*8*ϕ10mm
Steel transversal bars	Double sided

The effective width of cross-section beam was done according with EUROCODE 4 (2004) [3]. The Figure 2 illustrates the composite beam section and steel bars detail in the pre-fabricated concrete slab for the simple-sided specimens (TNRSS and TRSS). The Table 3 indicates the main material properties.

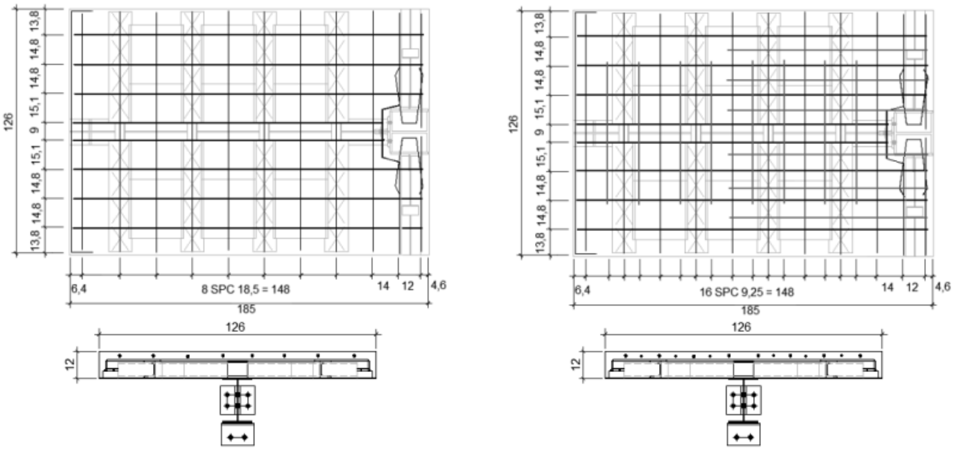

Figure 2: Steel bars details in the concrete slab and beam section.

Table 3: Material properties.

Element	f_y (kN/cm^2)	f_{max} (kN/cm^2)
Beam	36.41	45.12
Column	37.36	56.00
Bottom and web angle	39.70	47.80
Longitudinal steel bars	55.43	59.48
Concrete: f_{cm} = 18.9 MPa – TRSS and CRSS specimens		
f_{cm} = 39.2 MPa – TNRSS and CNRSS specimens		
where f_y = proportional limit stress and f_{max} = ultimate stress		

The same geometrical characteristics indicated in Table 2 and steel bars details illustrated in Figure 2 were adopted on the cruciform specimens (CNRSS and CRSS). The Figure 3 shows the general view of the TRSS and CRSS specimens.

Figure 3: TRSS and CRSS specimens general view.

3 NUMERICAL MODELING

In the numerical modeling, the most important step to construct a representative model is the finite element choice and the non-linearity of the materials representation, with the respective stress-strain relationship. It was adopted the FEM methodology (ANSYS program), with multi-linear diagram for the stress-strain relationship – Maggi (2004) [4], according with the Figure 4 for the bolts and steel plates, which can be simulated the plastic stage and pos-plastic effects on the steel components.

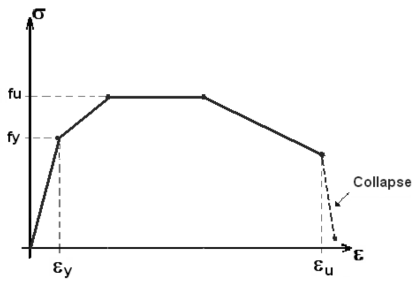

Bolts

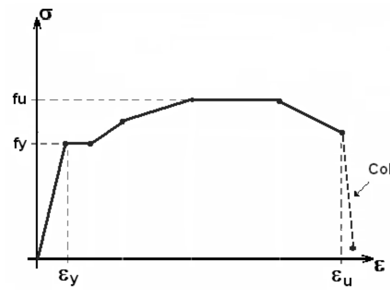

Steel plates

Figure 4: Stress-strain relationship for the bolts and steel plates.

In the concrete slab, it was adopted the stress-strain relationship showed in Figure 5 for compressive stress, according to the EUROCODE 2 (2003) [5], and shortening strain as absolute value for tension strain-stress relationship.

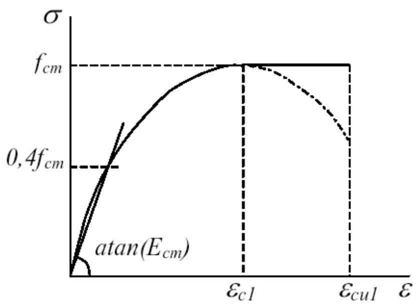

f_{cm} = mean value of the measured cylinder compressive strength of concrete.

ε_{c1} = strain at peak stress.

ε_{cu1} = ultimate strain in the compression

Figure 5: Stress-strain relationship for the concrete slab.

A 3D finite element was adopted for the beam, column, bolts and concrete slab components. The solid element in ANSYS software was chosen with the objective of representing volumetric elements. A 2D plastic element was adopted for the steel bars and shear connectors. The geometrical discontinuities were represented by contact elements. These elements work only when there is compression in the contact. Besides, large displacements were used in the numerical modeling. The Figure 6 illustrates the general view for beam to column composite connections with bottom and web angle and concrete slab. The Figure 7 shows the bolt meshes detail used for these analyses.

The initial stiffness of the numerical models depends on the bolts pre-load, the elastic material properties and the geometrical characteristics. The loading was applied in two phases: first a negative gradient temperature was considered to simulate the bolts pre-loaded; in a second phase, a vertical load was applied at the end of beam. The constitutive models are independent of applied temperatures and, therefore, the application of the temperature does not influence the non-linear constitutive laws.

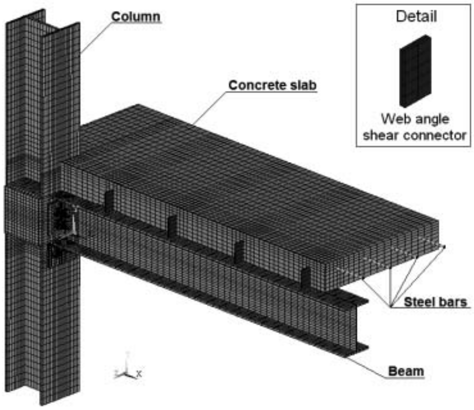

Figure 6: Complete numerical model.

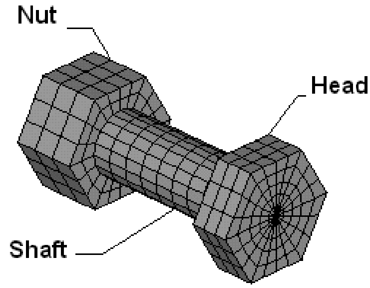

Figure 7: Bolt meshes detail.

4 RESULTS

The behavior of the beam-to-column connections crucially influences the overall frame response, which may be represented by moment-rotation (M-θ) relationship. The M-θ behaviors of numerical and experimental models are indicated in Figure 8 and Figure 9 for the single-sided and double-sided connections, respectively.

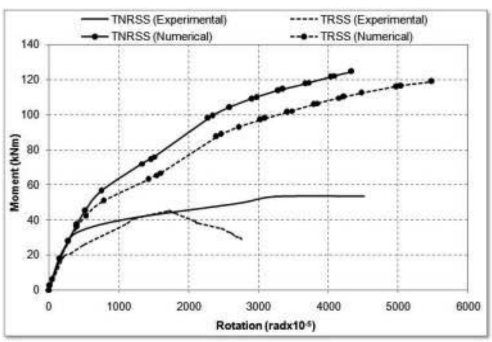

Figure 8: *M-θ* behavior for single sided connections.

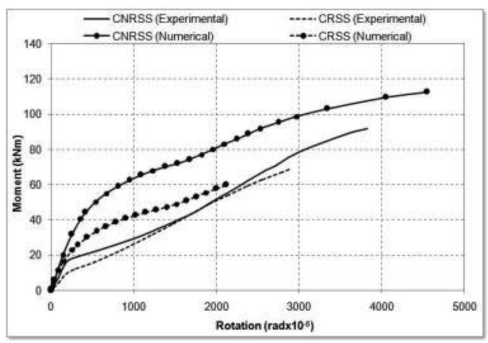

Figure 9: *M-θ* behavior for double sided connections.

Numerical initial stiffness showed a good agreement with experimental specimens, including similar results for connections with 0.2% and 1% for steel longitudinal bars ratio, with decrease of the resistant moment in the experimental specimens due to crack increasing in the slab concrete. The concrete slabs cracking next to the column are showed in the Figure 10 and Figure 11 for the TRSS and CRSS specimens, respectively.

Design value of the resistance moment of a composite section (M_{Rd}) and the initial stiffness are indicated in Table 4 for the analytical results (according to EUROCODE 3 (2005) [6]), numerical and experimental specimens. The resistance moment (M_{Rd}) corresponds to the connection maximum moment or the connection moment at the 20 rad.10^{-5} rotation.

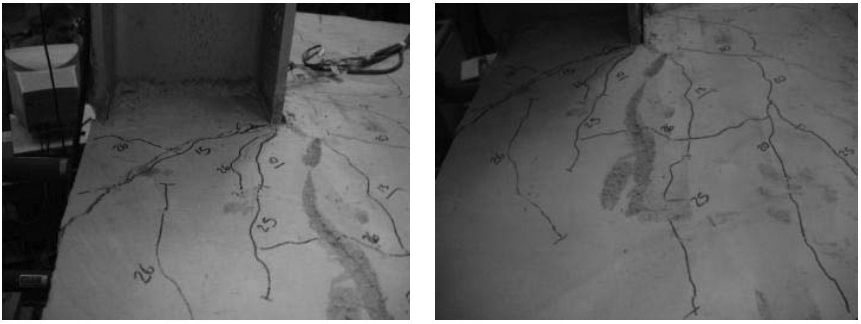

Figure 10: TRSS concrete slab cracking.

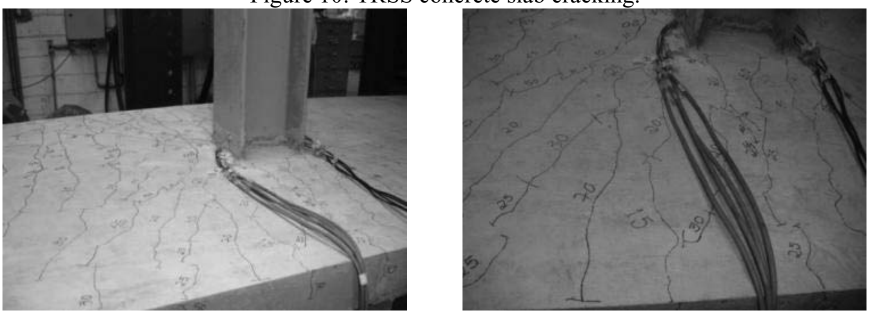

Figure 11: CRSS concrete slab cracking.

Table 4: General results.

Specimens	Parameter	Experimental (a)	Numerical (b)	Analytical (c)	(a)/(b)	(a)/(c)
TNRSS	M_{Rd} (kNm)	46.83	94.62	65.07	0.49	2.07
	$S_{j,ini}$ (kNm/rad)	10397.6	12143.8	12832.4	0.86	1.08
TRSS	M_{Rd} (kNm)	45.57	80.68	65.07	0.57	0.70
	$S_{j,ini}$ (kNm/rad)	8723.2	13686.79	12832.4	0.64	0.68
CNRSS	M_{Rd} (kNm)	51.81	80.04	65.07	0.65	0.08
	$S_{j,ini}$ (kNm/rad)	12835.2	14792.1	15295.1	0.87	0.48
CRSS	M_{Rd} (kNm)	50.93	59.17	65.07	0.86	0.78
	$S_{j,ini}$ (kNm/rad)	5456.5	13237.3	15295.1	0.41	0.37

According to the results, the single-sided and double-sided specimens presented reduced moment resistant due to cracking increasing in the concrete slab in the firsts steps loading. These effects can be imputed to the longitudinal steel bars anchorage no-efficiency in the isolated composite connections specimens.

On the other hand, the numerical modeling considers the effective longitudinal steel bars anchorage with, consequently, higher connection moment resistant compared with their respective specimens. The moment-rotation connection behavior can be predicted by [6], which proposed a simplified bi-linear or tri-linear design moment-rotation curve used in the frames analysis. The moment-rotation relationships are showed in the Figure 12 and Figure 13 for the single-sided and double-sided composite connections, respectively.

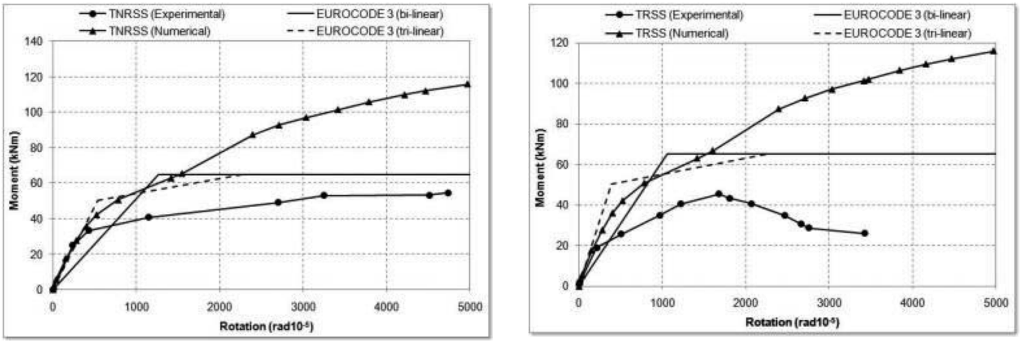

Figure 12: M-θ comparisons of single sided composite connections.

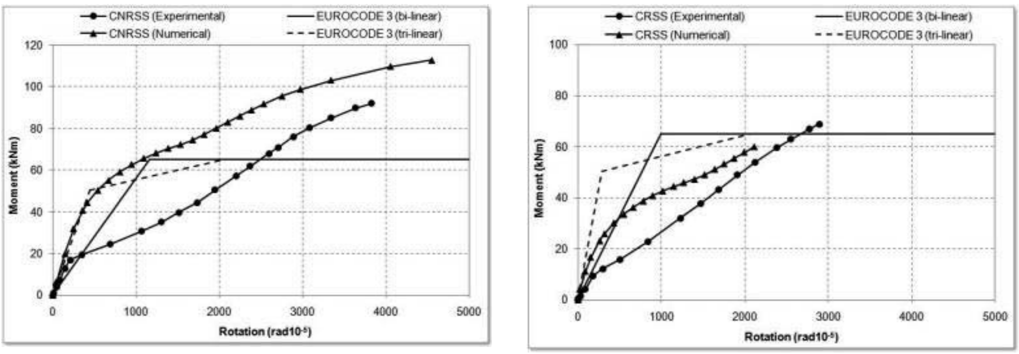

Figure 13: M-θ comparisons of double sided composite connections.

The Figure 14 illustrates the TRSS experimental prototype final displacement (numerical and experimental) at the 4.000.rad10^{-5} rotation.

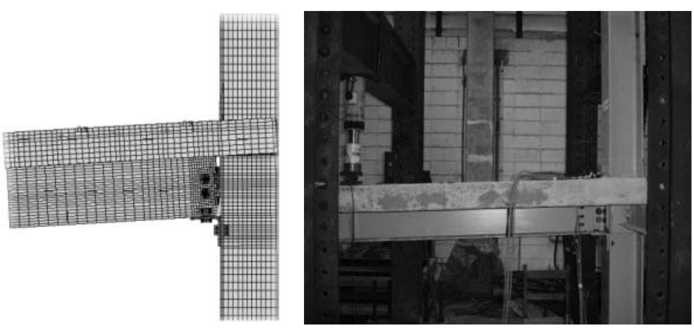

Figure 14: TRSS numerical and experimental specimen displacement at the 4.000.rad10^{-5} rotation.

5 CONCLUSIONS

The experimental specimens of beam-to-column composite connections were described and compared with analytical results and numerical modeling. The single-sided and double-sided specimens were fabricated with precast concrete slabs with steel joist (predalles) and bricks infill.

Numerical modeling allows the development of the concrete slab cracking and local stress concentration in the concrete slab and, the interactions among concrete slab, shear connectors and longitudinal steel bars. The numerical and experimental results were compared with the analytical results; obtained by the Component Method, for the composite steel concrete connections and represented satisfactorily the plastic mechanism and the ultimate limit states.

The proposed details to the longitudinal steel bars anchorage were not effective to reduce the cracking mechanism in the isolated concrete slab specimens due to the no-beam continuity through to the column minor axis.

REFERENCES

[1] Li, T.Q; Moore, D.B; Nethercot, D.A; Choo, B.S. "The Experimental behavior of a full-scalle semi-rigidly connected composite frame: Overall considerations". *Journal of Constructional Steel Research,* **39**(3):167-91, 1996.

[2] Bessa, W. O. "Theoretical and Experimental Analysis of Beam-to-Column Composite Connections with Bottom and Web Angle – Typical Floor and Isolated Prototypes". Ph. D. Thesis, Engineering School of São Carlos, University of São Paulo, São Carlos, Brazil (in Portuguese), 2009.

[3] EUROCODE 4 prEN 1994-1-1. "Design of Steel and Concrete Structures: Part 1-1: General Rules for Buildings". European Committee for Standartization, Brussels (final Draft), 2004.

[4] Maggi, Y. I. "Analysis of the structural behavior of bolted beam-column extended end plate connections." *Ph. D. Thesis, Engineering School of São Carlos, University of São Paulo*, São Carlos, Brazil (in Portuguese), 2004.

[5] EUROCODE 2 prEN 1992-1. "Design of Concrete Structures: Part 1-1: General Rules and Rules for Buildings". European Committee for Standartization, Brussels (final Draft), 2003.

[6] EUROCODE 3. "Design of Steel Joints: Part 1-8: General Rules". European Committee for Standartization, Brussels, 2005.

[7] Leon, R.T. "Semi-Rigid Composite Construction." *Journal of Constructional Steel Research*, **25**: 99-120, 1990.

[8] Calado, L. and Castiglioni, C. A. "Steel beam-to-column connections under low-cyclic fatigue experimental and numerical research." Proceedings of XI Word Conference on Earthquake Engineering, Acapulco, Mexico, 1996.

[9] Wan, J.F and Li, G. Q. "Testing of semi-rigid steel-concrete composite frames subjected to vertical loads." *Engineering Structures*. In press, corrected proof, November, 2006.

[10] Ahmed, B. and Nethercot, D. A. "Prediction of initial stiffness and available rotation capacity of major-axis flush end-plate connections." *Journal of Constructional Steel Research*, **41(1)**: 31-60, 1997.

[11] Li, T.Q; Choo, B.S. and Nethercot, D. A. "Determination of rotation capacity requirements for the steel composite beams." *Journal of Constructional Steel Research*, **32**: 303-32, 1995.